OL | Organic Letters

pubs.acs.org/OrgLett Letter

Iron-Catalyzed Photoredox Functionalization of Methane and Heavier Gaseous Alkanes: Scope, Kinetics, and Computational Studies

Qingqing Zhang, Shuyang Liu, Jinglan Lei, Yongqiang Zhang, Changgong Meng, Chunying Duan, and Yunhe Jin*

Cite This: *Org. Lett.* 2022, 24, 1901−1906 Read Online

ACCESS | Metrics & More | Article Recommendations | Supporting Information

ABSTRACT: Herein, we report the development of the photocatalytic C−H functionalization of methane, ethane, and heavier gaseous alkanes with good yields and selectivity, broad scope (57 examples), mild conditions, and low cost. Kinetics and density functional theory calculations were investigated for the key photoinduced ligand-to-metal charge transfer and hydrogen atom transfer processes to reveal the detailed mechanism of iron photocatalysis. This work may bring novel ideas for feedstock upgrading and catalyst design.

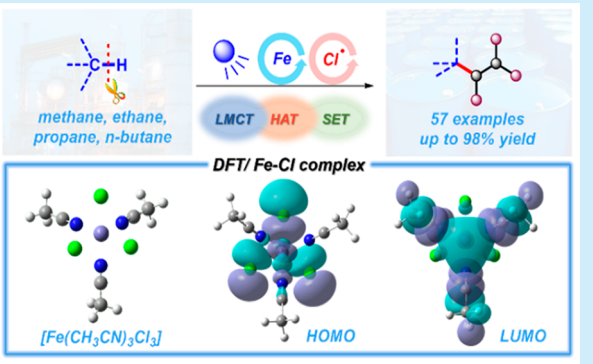

Gaseous alkanes, especially methane, are among the most abundant and low-cost organic carbon sources and are usually applied as fuels for heating, propulsion, or electricity generation.[1] However, both methane leakage during extraction and transportation and carbon dioxide emissions from alkane combustion result in the painful and disruptive effects of global warming.[2] In addition to these uses, methane and heavier analogues could also be employed as chemical feedstocks for high value-added synthesis without the need for functionalized reagents, bringing enormous economic and ecological benefits as well as great scientific challenges.[3] These challenges include, but are not limited to, the intrinsic inertness and high bond dissociation energies (BDEs) of C(sp^3)−H bonds (98.1−105.3 kcal/mol[4]) (Scheme 1a) and poor solubility of the gases in most solvents.[3c−e] In recent decades, significant progress has been made in producing methanol from methane.[3d,5] However, the vast majority of these transformations are carried out under heterogeneous conditions with additional well-known problems in terms of selectivity and high temperature.[5a,b] Significantly, reports on the production of different methyl-containing derivatives, instead of methanol with methane and a homogeneous catalyst, are rare and remain largely underdeveloped.[3d]

Photoinduced hydrogen atom transfer (HAT) catalysis has attracted much attention as one of the most environmentally friendly and efficient protocols for affording carbon-centered radicals from unactivated alkanes.[6] However, little effort has been devoted to the valuable functionalization of methane and other gaseous alkanes with this strategy.[7] Photodissociation of molecular chlorine is an effective approach to initiate methane halogenation in old processes; however, both the low yield and uncontrollable overfunctionalization of radical chain reactions and the use of toxic and corrosive molecular chlorine result in significant application limitations (Scheme 1b). Recently, the Zuo,[7b] Noël,[7d] and Schelter[7e] groups made remarkable breakthroughs in light-driven methane-functionalizing reactions via homogeneous catalysis (Scheme 1c); to a certain degree, the high oxidation potentials of photocatalysts and moderate yields (38−66%) restrict the further development and industrial application of these systems.

Iron, the most abundant transition metal element in the Earth's crust, has secured its place in photoinduced C−H activation of alkanes with a chlorine radical generated from the ligand-to-metal charge transfer (LMCT) process of an Fe−Cl complex.[7f,8] Based on our previous work[7f] and basic theories of photocatalysis[9] and iron catalysis,[10] the proposed mechanism of this efficient and sustainable system has been preliminarily established, as shown in Scheme 1c. The catalytic cycle starts at the photoexcitation of iron complex **A** near 365 nm (demonstrated by studies on UV−vis spectra[7f]), generating its

Received: January 21, 2022
Published: March 7, 2022

https://doi.org/10.1021/acs.orglett.2c00224
Org. Lett. 2022, 24, 1901−1906

Scheme 1. Photoinduced C(sp^3)−H Activation of Gaseous Hydrocarbons

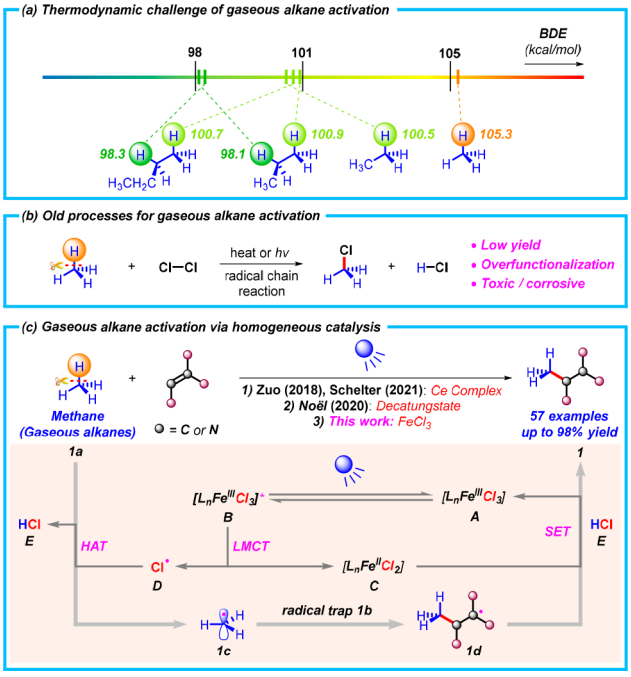

excited state **B**. The subsequent LMCT affords ferrous complex **C** and chlorine radical **D**. **D**, as a wonderful HAT catalyst, can activate the alkane substrate to carbon radical **1c**, followed by a radical trapping process between **1c** and radical trap **1b** to give another carbon radical **1d**. Finally, a single electron transfer (SET) takes place from **C** to **1d**, providing final product **1** and regenerating catalyst **A**. Considering that the development of this green and practical catalysis still has large potential in extra functionalizing reaction types and industrial applications, further studies aimed at obtaining comprehensive insight into the mechanism are essential. Furthermore, the scope of gaseous alkane functionalization through this strategy is quite limited. As an extension of our continuous interest in light-driven synthetic reactions,[7f,g,11] we embarked on enriching the substrate scope among gaseous hydrocarbons and performed kinetic and computational investigations on the detailed mechanism of iron photocatalysis.

Among all volatile hydrocarbons, methane is undoubtedly the most challenging to activate due to the high BDE of CH_3−H bonds (up to 105.3 kcal/mol[4]) but is also the most valuable because of its wide distribution and large reserves. Moreover, the success in the cleavage of methane bonds through our approach will make the splitting of C−H bonds of other gaseous aliphatic feedstocks within reach. Although the BDE of Cl−H bonds (103 kcal/mol[4]) is slightly lower than that of CH_3−H bonds, the successful activation of methane in old processes via a chlorine radical instills confidence in us. Initially, the model reaction between methane (**1a**) and 2-benzylidenemalononitrile (0.1 M) (**1b**) was performed with 0.1 equiv of $FeCl_3·6H_2O$ as the catalyst in CH_3CN under ambient methane pressure and light irradiation, affording the corresponding addition product **1** in only 8% yield with a messy system (entry 1 in Scheme 2). Increasing the methane pressure to 5 MPa gave an obviously improved but still moderate yield (entry 2). The undetected byproducts may

Scheme 2. Scope of Methane Functionalization[a]

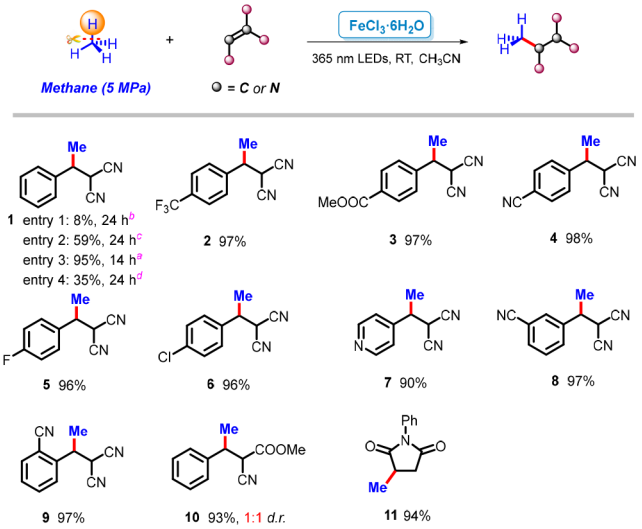

[a]Standard conditions for methane functionalization: radical trap (1 equiv., 0.02 M), $FeCl_3·6H_2O$ (0.1 equiv), CH_3CN (1 mL), temperature (rt, ~25 °C), 5 MPa methane pressure, 70 W 365 nm LEDs, 7−14 h reaction time (for more details, see the Supporting Information). Yields were determined by ^{1}H NMR analysis with an internal standard; *d.r.* value was determined by ^{1}H NMR analysis. [b]Radical trap (0.1 M), methane pressure (0.1 MPa). [c]Radical trap (0.1 M). [d]Irradiation with 30 W 405 nm LEDs.

include products from hydrogenation or $NCCH_2$−H bond activation, while d_3-acetonitrile was employed to partly avoid the formation of byproducts based on previous reports.[7b,d,e] Impressively, without similar concerns, our iron-catalyzed method was able to acquire **1** with normal acetonitrile in an excellent yield (up to 95%) just by lowering the substrate concentration of **1b**, which meant increasing the relative concentration of methane (entry 3). With the optimized conditions in hand (for more details on optimization of reaction conditions, see entry 4 and Table S4), the scope of methane functionalization was explored next (Scheme 2). Multifarious electronically distinct benzylidenemalononitriles were tested first, and all showed great efficiency (**1**−**9**). Many cross-coupling-useful functional groups, such as halogeno (**5**, **6**), cyano (**4**, **8**, **9**), and ester (**3**) groups, and biocompatible building blocks, such as trifluoromethyl (**2**) and pyridyl (**7**) groups, were involved at different substituted positions, demonstrating the good functional group tolerance and utilization potential of this reaction. In addition, two synthetically practical feedstocks (**10** and **11**) were obtained in excellent yields with methyl 2-cyano-3-phenylacrylate and *N*-phenylmaleimide as radical traps, respectively.

Sequentially, the functionalization scope of ethane, which is isolated from natural gas or petrochemical byproducts of petroleum refining, was examined (Scheme 3). Due to the higher solubility of ethane in acetonitrile than that of methane, the reactions could proceed efficiently in regular tubes under atmospheric pressure. Various benzylidenemalononitriles were tested first, and we obtained similar excellent results relative to methane (**12**−**23**). Many other types of hydroethylated compounds (**24**−**29**) were also provided in moderate to good yields with different radical traps. Furthermore, with a complicated substrate prepared from *glycylglycine*, the method displayed moderate reactivity toward the naturally sourced

https://doi.org/10.1021/acs.orglett.2c00224
Org. Lett. 2022, 24, 1901−1906

Scheme 3. Scope of Ethane, Propane, and *n*-Butane Functionalization[a]

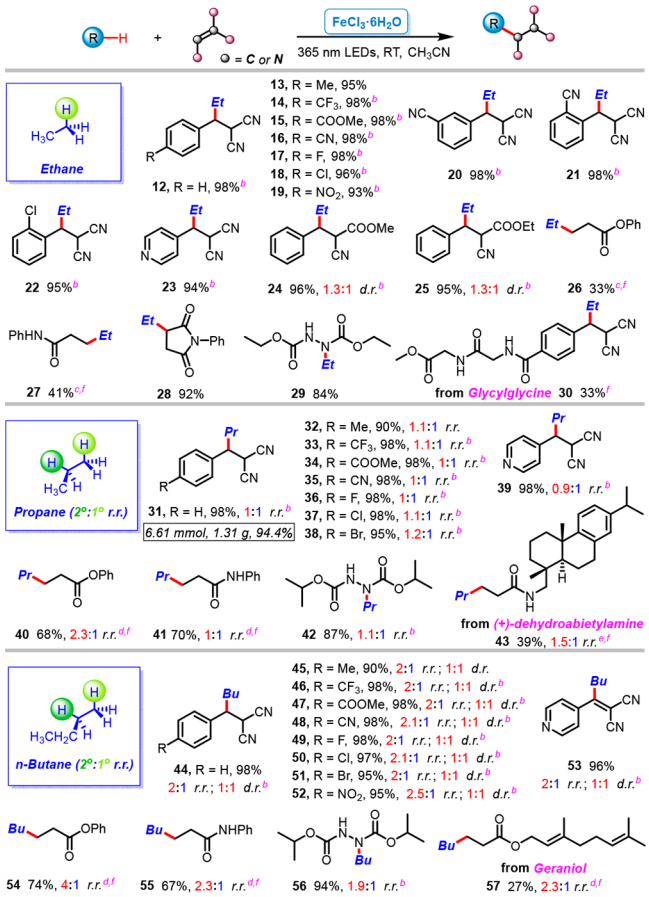

[a]Standard conditions for ethane, propane and *n*-butane functionalization: radical trap (1 equiv., 0.1 mmol), $FeCl_3·6H_2O$ (0.03 equiv), CH_3CN (3 mL), temperature (rt, ~25 °C), 0.1 MPa pressure, 30 W, 365 nm LEDs, and 0.5−12 h reaction time (for more details, see the Supporting Information). Yields were determined by ^1H NMR analysis with an internal standard; *d.r.* and *r.r.* values were determined by ^1H NMR analysis or GC−MS analysis. [b]The pure products were obtained by aqueous washing without chromatography. [c]$FeCl_3·6H_2O$ (0.1 equiv), CH_3CN (5 mL), 2 MPa pressure. [d]$FeCl_3·6H_2O$ (0.1 equiv). [e]$FeCl_3·6H_2O$ (0.5 equiv). [f]Yields were determined by ^1H NMR analysis with internal standard after isolation.

example (**30**). Next, a similar research strategy was performed to extend the substrate scope for propane and *n*-butane, the major components of liquid petroleum gas (LPG) (Scheme 3). The reactions retained good to excellent efficiency in generating the corresponding hydroalkylation products (**31**−**42**, **44**−**56**). The reaction yield did not obviously decrease in gram-scale synthesis (**31**). Further studies on the regiomeric ratios (*r.r.*) of target products at different positions of alkanes (such as 1:1 for **31**, 2:1 for **44**) suggested that the regioselectivities were mainly determined by different transition state energies of HAT progressing in situ (2°/1°) and quantities of hydrogens with the same chemical environment.[7f,12] Another two naturally sourced samples from (+)-*dehydroabietylamine* and *geraniol* were synthesized as well and exhibited moderate reaction yields (**43**, **57**), further highlighting the potential utility of this approach for late-stage modification of complex molecules. Three typical examples for liquid alkanes (**58**−**60**) were also attempted as substrates, and great reaction yields were obtained (Table S5). Importantly, with the pursuit of practical and sustainable chemistry, most desired pure products could be achieved with a simple aqueous wash without chromatography because of the superb conversion rate of the substrates to products and the water-soluble ferric catalyst as the only additive. The reaction residue of this system exhibited slightly acidic based on the pH of the reaction detected as 3.7 after being diluted 10-fold with water. Meanwhile, we also tried some unactivated olefins and electron-rich alkenes as radical traps and found that they did not work well in this system (Table S6).

The kinetic experiments were conducted on three model reactions (**1**, **4**, and **5**) to gain deep insights into the mechanism of iron-catalyzed methane activation (Scheme 4a−c, for more details see Tables S1−S3). First, the kinetic profiles of methane pressure are presented in Scheme 4a. A linear relationship between the first-hour yields (related to initial reaction rates) and methane pressure from 0.1 to 3 MPa was observed, which implied a first-order dependence on methane concentration in solvent. The lost linear relationship under pressures over 3 MPa may have resulted from the decreasing concentration of substrate and the high-pressure effect that influenced the solubility of gas.[13] A positive but nonlinear correlation between the first-hour yields and iron catalyst loading was revealed next (Scheme 4b), exhibiting that both methane and catalyst concentrations contributed positively to the formation of hydromethylation products. Finally, no exponential upward trend was found in the time curves of the three model reactions (Scheme 4c), which suggested that radical chain reactions made little contribution in this system, contrary to old processes. The quantum yield of the **1**-generating reaction was also measured as 0.0015 ≪ 1 to further prove this issue (for more details, see Scheme S1).[14]

Using the reaction of methane and **1b** as a representative, density functional theory (DFT) and time-dependent DFT (TDDFT) calculations (for computational details, see the Supporting Information) were carried out to dissect the reaction pathway (Scheme 4d−f). First, to recognize the real iron complex that was photoexcited and launched the reaction, we predicted the UV−vis spectra of $FeCl_3(CH_3CN)_3$, $[FeCl_2(CH_3CN)_4]^+$, and $[FeCl(CH_3CN)_5]^{2+}$ (Figures S9−S11), in which the spectrum of $FeCl_3(CH_3CN)_3$ (**A**) matched accurately with the experimental spectrum of $FeCl_3·6H_2O$ dissolved in CH_3CN at the characteristic absorption peaks near 315 and 365 nm (Scheme 4d). Sequentially, the detailed excitation states of **A** were calculated (Table S7). The tiny differences in excitation levels led to high rates of internal conversion, supporting all of the deexcitation processes occurring at the S_1 state (**B**) according to Kasha's rule.[15] **B** was proposed to be a long-lifetime state due to the attenuated radiative transition resulting from its C_3 axial symmetry and oscillator strength calculated as 0. In addition, the examination of the HOMO and LUMO of **A** (Figures S12 and S13) provided the possibility for undergoing the desired LMCT from Cl^- to Fe(III) with the long-lifetime excitation. More evidence was supplied by calculation of the charge density difference (CDD) of **B** (Scheme 4e), reflecting **B** to be a typical charge-transfer state with electrons predominantly localized to Fe and holes localized to Cl. As a result, the holes induced by photoexcitation could oxidize Cl^- to HAT-active Cl radicals. Analysis of the Gibbs free energy change with optimized structures was conducted in three stages (Scheme 4f). For the LMCT stage, the excitation energy of **B**

https://doi.org/10.1021/acs.orglett.2c00224
Org. Lett. 2022, 24, 1901−1906

Scheme 4. Kinetic Studies and Computational Investigations

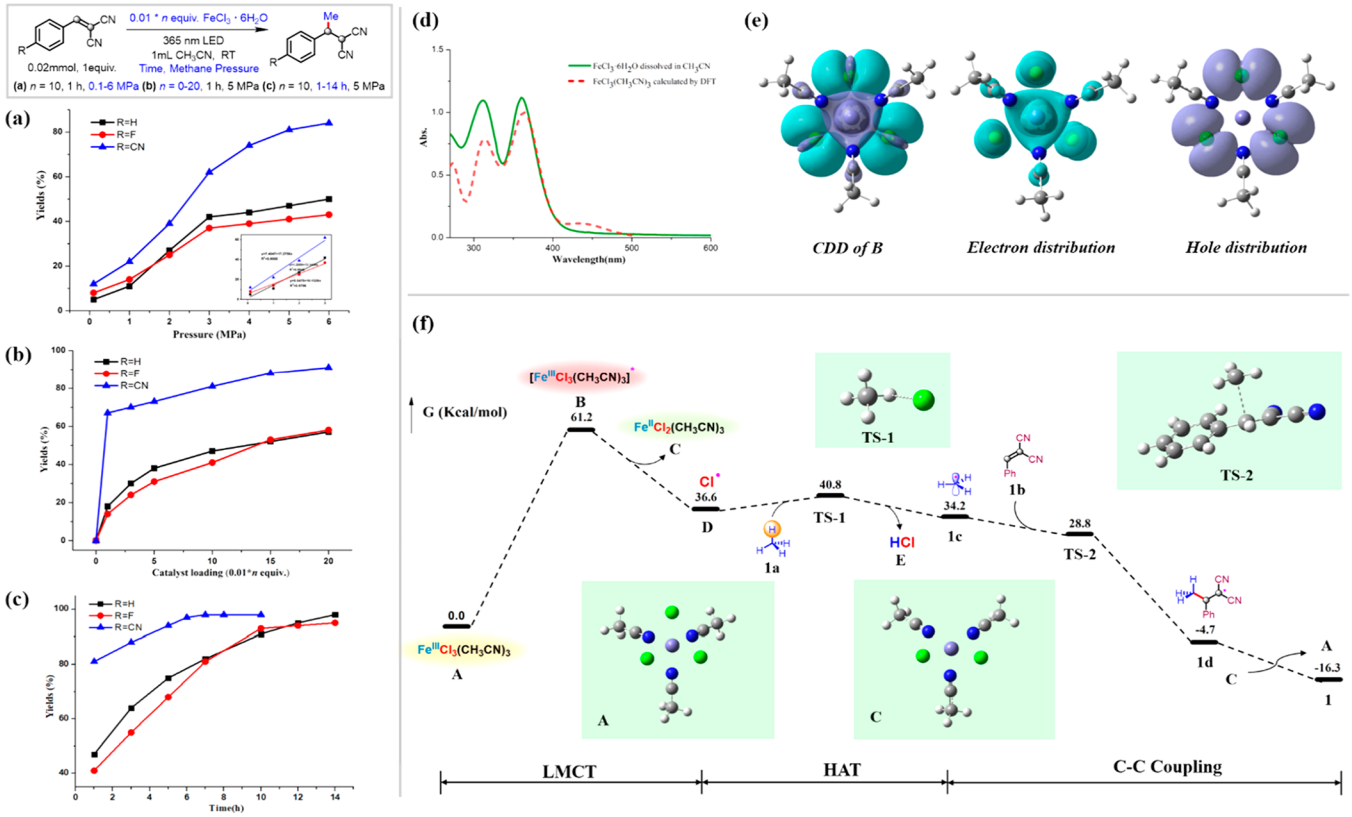

(61.2 kcal/mol) was higher than the free energy change from **A** to **C** and **D** (36.6 kcal/mol), proving that the process takes place according to thermodynamic law. For the HAT stage, the weak free energy change from **D** to **1c** (−2.4 kcal/mol) was responsible for the difficulty and low reaction rate during methane activation. Furthermore, the large gap between the two energy barriers (**A** → **B** vs **D** → **Ts-1**) should verify that the photoexcitation of **A** is the "rate-determining step" while the C−H activation step is just the "product-determining step".[7f] The production of alkyl radicals was also proved by radical trapping experiments (for more details, see Figure S8). Only a negative transition state[16] with no energy barrier was observed when we scanned the whole potential energy surface of the last C−C coupling stage, confirming that the reaction completed spontaneously. This result further reflected the strong radical-capture ability of **1b**, which was responsible for the significant yield and the uniqueness of this kind of radical trap for this reaction.

Given the easy accessibility and low cost of the photocatalyst and substrates, mild reaction conditions, large scope with natural product fragments involved, and convenience of purification, we believe that the highly efficient, green, and concise system outlined herein is ideal from the vantage point of feedstock upgrading. Deep insights into the LMCT and subsequent HAT processes and the importance of solvent effects with kinetic and computational studies may offer intriguing opportunities for expanding transition types and commercial application of simple hydrocarbon functionalization and for novel inspiration for further design of photocatalysts and catalytic systems.

■ ASSOCIATED CONTENT

Supporting Information

The Supporting Information is available free of charge at https://pubs.acs.org/doi/10.1021/acs.orglett.2c00224.

Mechanism investigations, synthetic procedures, characterization data and ^{1}H and ^{13}C NMR spectra of these synthesized compounds (PDF)

■ AUTHOR INFORMATION

Corresponding Author

Yunhe Jin − *State Key Laboratory of Fine Chemicals, Zhang Dayu School of Chemistry, Dalian University of Technology, Dalian 116024, China;* orcid.org/0000-0003-0626-4587; Email: jinyh18@dlut.edu.cn

Authors

Qingqing Zhang − *State Key Laboratory of Fine Chemicals, Zhang Dayu School of Chemistry, Dalian University of Technology, Dalian 116024, China*

Shuyang Liu − *State Key Laboratory of Fine Chemicals, Zhang Dayu School of Chemistry, Dalian University of Technology, Dalian 116024, China*

Jinglan Lei − *State Key Laboratory of Fine Chemicals, Zhang Dayu School of Chemistry, Dalian University of Technology, Dalian 116024, China*

Yongqiang Zhang − *State Key Laboratory of Fine Chemicals, Zhang Dayu School of Chemistry, Dalian University of Technology, Dalian 116024, China*

Changgong Meng − *State Key Laboratory of Fine Chemicals, Zhang Dayu School of Chemistry, Dalian University of*

https://doi.org/10.1021/acs.orglett.2c00224
Org. Lett. 2022, 24, 1901−1906

Technology, Dalian 116024, China; orcid.org/0000-0003-1662-0565

Chunying Duan − *State Key Laboratory of Fine Chemicals, Zhang Dayu School of Chemistry, Dalian University of Technology, Dalian 116024, China;* orcid.org/0000-0003-1638-6633

Complete contact information is available at: https://pubs.acs.org/10.1021/acs.orglett.2c00224

Notes

The authors declare no competing financial interest.

■ ACKNOWLEDGMENTS

The authors would like to thank Dr. Haifang Li at Tsinghua University for her great help with the analysis of high-resolution mass spectrometry. We acknowledge the support of the National Natural Science Foundation of China (21901032, 21890381, 21820102001) and the Fundamental Research Funds for the Central Universities (DUT21LK13).

■ REFERENCES

(1) (a) Kerr, R. A. Natural Gas From Shale Bursts Onto the Scene. *Science* **2010**, *328*, 1624−1626. (b) Cooper, J.; Stamford, L.; Azapagic, A. Shale Gas: A Review of the Economic, Environmental, and Social Sustainability. *Energy Technol.* **2016**, *4*, 772−792.

(2) Control methane to slow global warming - fast. *Nature* **2021**, *596*, 461−461.

(3) (a) Shilov, A. E.; Shul'pin, G. B. Activation of C-H bonds by metal complexes. *Chem. Rev.* **1997**, *97*, 2879−2932. (b) Das, J.; Guin, S.; Maiti, D. Diverse strategies for transition metal catalyzed distal C(sp^3)-H functionalizations. *Chem. Sci.* **2020**, *11*, 10887−10909. (c) Caballero, A.; Perez, P. J. Methane as raw material in synthetic chemistry: the final frontier. *Chem. Soc. Rev.* **2013**, *42*, 8809−8820. (d) Gunsalus, N. J.; Koppaka, A.; Park, S. H.; Bischof, S. M.; Hashiguchi, B. G.; Periana, R. A. Homogeneous Functionalization of Methane. *Chem. Rev.* **2017**, *117*, 8521−8573. (e) Pulcinella, A.; Mazzarella, D.; Noel, T. Homogeneous catalytic C(sp^3)-H functionalization of gaseous alkanes. *Chem. Commun.* **2021**, *57*, 9956−9967.

(4) Luo, Y.-R. *Comprehensive Handbook of Chemical Bond Energies*; CRC Press: Boca Raton, FL, 2007.

(5) For selected reviews, see: (a) Ravi, M.; Ranocchiari, M.; van Bokhoven, J. A. The Direct Catalytic Oxidation of Methane to Methanol-A Critical Assessment. *Angew. Chem., Int. Ed.* **2017**, *56*, 16464−16483. (b) Tang, P.; Zhu, Q.; Wu, Z.; Ma, D. Methane activation: the past and future. *Energy Environ. Sci.* **2014**, *7*, 2580−2591. (c) Cavaliere, V. N.; Wicker, B. F.; Mindiola, D. J. Chapter one−homogeneous organometallic chemistry of methane. *Adv. Organomet. Chem.* **2012**, *60*, 1−47.

(6) (a) Capaldo, L.; Ravelli, D. Hydrogen Atom Transfer (HAT): A Versatile Strategy for Substrate Activation in Photocatalyzed Organic Synthesis. *Eur. J. Org. Chem.* **2017**, *2017*, 2056−2071. (b) Rohe, S.; Morris, A. O.; McCallum, T.; Barriault, L. Hydrogen atom transfer reactions via photoredox catalyzed chlorine atom generation. *Angew. Chem., Int. Ed.* **2018**, *57*, 15664−15669. (c) Ravelli, D.; Fagnoni, M.; Fukuyama, T.; Nishikawa, T.; Ryu, I. Site-Selective C-H Functionalization by Decatungstate Anion Photocatalysis: Synergistic Control by Polar and Steric Effects Expands the Reaction Scope. *ACS Catal.* **2018**, *8*, 701−713. (d) Huang, C.; Wang, J.-H.; Qiao, J.; Fan, X.-W.; Chen, B.; Tung, C.-H.; Wu, L.-Z. Direct arylation of unactivated alkanes with heteroarenes by visible-light catalysis. *J. Org. Chem.* **2019**, *84*, 12904−12912. (e) Huang, C. Y.; Li, J.; Liu, W.; Li, C. J. Diacetyl as a "traceless" visible light photosensitizer in metal-free cross-dehydrogenative coupling reactions. *Chem. Sci.* **2019**, *10*, 5018−5024. (f) Zhao, H.; Jin, J. Visible Light-Promoted Aliphatic C-H Arylation Using Selectfluor as a Hydrogen Atom Transfer Reagent. *Org. Lett.* **2019**, *21*, 6179−6184. (g) Li, G.-X.; Hu, X.; He, G.; Chen, G. Photoredox-Mediated Minisci-type Alkylation of N-Heteroarenes with Alkanes with High Methylene Selectivity. *ACS Catal.* **2018**, *8*, 11847−11853. (h) Shao, X.; Wu, X.; Wu, S.; Zhu, C. Metal-Free Radical-Mediated C(sp^3)-H Heteroarylation of Alkanes. *Org. Lett.* **2020**, *22*, 7450−7454. (i) Xu, P.; Chen, P. Y.; Xu, H. C. Scalable Photoelectrochemical Dehydrogenative Cross-Coupling of Heteroarenes with Aliphatic C-H Bonds. *Angew. Chem., Int. Ed.* **2020**, *59*, 14275−14280. (j) Shields, B. J.; Doyle, A. G. Direct C(sp^3)-H cross coupling enabled by catalytic generation of chlorine radicals. *J. Am. Chem. Soc.* **2016**, *138*, 12719−12722. (k) Treacy, S. M.; Rovis, T. Copper Catalyzed C(sp^3)-H Bond Alkylation via Photoinduced Ligand-to-Metal Charge Transfer. *J. Am. Chem. Soc.* **2021**, *143*, 2729−2735.

(7) (a) Ohkubo, K.; Hirose, K. Light-Driven C-H Oxygenation of Methane into Methanol and Formic Acid by Molecular Oxygen Using a Perfluorinated Solvent. *Angew. Chem., Int. Ed.* **2018**, *57*, 2126−2129. (b) Hu, A.; Guo, J.-J.; Pan, H.; Zuo, Z. Selective functionalization of methane, ethane, and higher alkanes by cerium photocatalysis. *Science* **2018**, *361*, 668−672. (c) Deng, H.-P.; Zhou, Q.; Wu, J. Microtubing-reactor-assisted aliphatic C-H functionalization with HCl as a hydrogen-atom-transfer catalyst precursor in conjunction with an organic photoredox catalyst. *Angew. Chem., Int. Ed.* **2018**, *57*, 12661−12665. (d) Laudadio, G.; Deng, Y.; van der Wal, K.; Ravelli, D.; Nuño, M.; Fagnoni, M.; Guthrie, D.; Sun, Y.; Noël, T. C(sp^3)-H functionalizations of light hydrocarbons using decatungstate photocatalysis in flow. *Science* **2020**, *369*, 92−96. (e) Yang, Q.; Wang, Y.-H.; Qiao, Y.; Gau, M.; Carroll, P. J.; Walsh, P. J.; Schelter, E. J. Photocatalytic C-H activation and the subtle role of chlorine radical complexation in reactivity. *Science* **2021**, *372*, 847−852. (f) Jin, Y.; Zhang, Q.; Wang, L.; Wang, X.; Meng, C.; Duan, C. Convenient C(sp^3)-H bond functionalisation of light alkanes and other compounds by iron photocatalysis. *Green Chem.* **2021**, *23*, 6984−6989. (g) Zhang, Y.; Jin, Y.; Wang, L.; Zhang, Q.; Meng, C.; Duan, C. Selective C(sp^3)-H activation of simple alkanes: visible light-induced metal-free synthesis of phenanthridines with H_2O_2 as a sustainable oxidant. *Green Chem.* **2021**, *23*, 6926−6930.

(8) (a) Shul'pin, G. B.; Nizova, G. V.; Kozlov, Y. N. Photochemical aerobic oxidation of alkanes promoted by iron complexes. *New. J. Chem.* **1996**, *20*, 1243−1256. (b) Wu, W.; Fu, Z.; Wen, X.; Wang, Y.; Zou, S.; Meng, Y.; Liu, Y.; Kirk, S. R.; Yin, D. Light-triggered oxychlorination of cyclohexane by metal chlorides. *Appl. Catal. A-Gen.* **2014**, *469*, 483−469. (c) Kang, Y. C.; Treacy, S. M.; Rovis, T. Iron-Catalyzed Photoinduced LMCT: A 1° C-H Abstraction Enables Skeletal Rearrangements and C(sp^3)−H Alkylation. *ACS Catal.* **2021**, *11*, 7442−7449.

(9) For selected reviews, see: (a) Stephenson, C. R. J.; Yoon, T. P.; MacMillan, D. W. C. *Visible Light Photocatalysis in Organic Chemistry*; Wiley, 2018. (b) Skubi, K. L.; Blum, T. R.; Yoon, T. P. Dual catalysis strategies in photochemical synthesis. *Chem. Rev.* **2016**, *116*, 10035−10074. (c) Romero, N. A.; Nicewicz, D. A. Organic photoredox catalysis. *Chem. Rev.* **2016**, *116*, 10075−10166.

(10) For selected reviews, see: (a) Huang, X.; Groves, J. T. Beyond ferryl-mediated hydroxylation: 40 years of the rebound mechanism and C-H activation. *J. Biol. Inorg. Chem.* **2017**, *22*, 185−207. (b) Liu, Y.; You, T.; Wang, H.-X.; Tang, Z.; Zhou, C.-Y.; Che, C.-M. Iron- and cobalt-catalyzed C(sp^3)-H bond functionalization reactions and their application in organic synthesis. *Chem. Soc. Rev.* **2020**, *49*, 5310−5358.

(11) (a) Jin, Y.; Ou, L.; Yang, H.; Fu, H. Visible-light-mediated aerobic oxidation of N-alkylpyridinium salts under organic photocatalysis. *J. Am. Chem. Soc.* **2017**, *139*, 14237−14243. (b) Jin, Y.; Yang, H.; Fu, H. An N-(acetoxy)phthalimide motif as a visible-light pro-photosensitizer in photoredox decarboxylative arylthiation. *Chem. Commun.* **2016**, *52*, 12909−12912. (c) Jin, Y.; Yang, H.; Fu, H. Thiophenol-catalyzed visible-light photoredox decarboxylative couplings of N-(acetoxy)phthalimides. *Org. Lett.* **2016**, *18*, 6400−6403. (d) Jin, Y.; Zhang, Q.; Zhang, Y.; Duan, C. Electron transfer in the confined environments of metal-organic coordination supramolecular systems. *Chem. Soc. Rev.* **2020**, *49*, 5561−5600. (e) Jin, Y.; Fu, H.

Visible-light photoredox decarboxylative couplings. *Asian J. Org. Chem.* **2017**, *6*, 368−385.
(12) An, Q.; Wang, Z.; Chen, Y.; Wang, X.; Zhang, K.; Pan, H.; Liu, W.; Zuo, Z. Cerium-catalyzed C−H functionalizations of alkanes utilizing alcohols as hydrogen atom transfer agents. *J. Am. Chem. Soc.* **2020**, *142*, 6216−6226.
(13) Atkins, P.; de Paula, J. *Physical Chemistry*; Oxford University Press: Oxford, 2014.
(14) Cismesia, M. A.; Yoon, T. P. Characterizing chain processes in visible light photoredox catalysis. *Chem. Sci.* **2015**, *6*, 5426−5434.
(15) Kasha, M. Characterization of electronic transitions in complex molecules. *Discuss. Faraday Soc.* **1950**, *9*, 14−19.
(16) (a) Zhao, Y.-X.; Wu, X.-N.; Ma, J.-B.; He, S.-G.; Ding, X.-L. Experimental and Theoretical Study of the Reactions between Vanadium-SiliconHeteronuclear Oxide Cluster Anions with N-Butane. *J. Phys. Chem. C* **2010**, *114*, 12271−12279. (b) Feyel, S.; Döbler, J.; Hoeckendorf, R.; Beyer, M. K.; Sauer, J.; Schwarz, H. Activation of Methane by Oligomeric $[(Al_2O_3)_X^+$ (X = 3,4,5)]: TheRole of Oxygen-Centered Radicals in Thermal Hydrogen-Atom Abstraction. *Angew. Chem., Int. Ed.* **2008**, *47*, 1946−1950.

https://doi.org/10.1021/acs.orglett.2c00224
Org. Lett. 2022, 24, 1901−1906